Sensitized Hole Injection of Phosphorus Porphyrin into NiO: Toward New Photovoltaic Devices

Magnus Borgström,[†] Errol Blart,[‡] Gerrit Boschloo,[§] Emad Mukhtar,[†] Anders Hagfeldt,[§] Leif Hammarström,*[,†] and Fabrice Odobel*[,‡]

Department of Physical Chemistry, Uppsala University, Box 579, SE-751 23 Uppsala, Sweden, Laboratoire de Synthèse Organique, UMR 6513 CNRS & FR CNRS 2465, Université de Nantes, Faculté des Sciences et des Techniques de Nantes, BP 92208 2, rue de la Houssinière, 44322 Nantes Cedex 03, France, and Center of Molecular Devices, Department of Chemistry, Physical Chemistry, Royal Institute of Technology (KTH), Teknikringen 30, 100 44 Stockholm, Sweden

Received: July 21, 2005; In Final Form: October 7, 2005

This paper describes the preparation and the characterization of a photovoltaic cell based on the sensitization of a wide band gap p-type semiconductor (NiO) with a phosphorus porphyrin. A photophysical study with femtosecond transient absorption spectroscopy showed that light excitation of the phosphorus porphyrin chemisorbed on NiO particles induces a very rapid interfacial hole injection into the valence band of NiO, occurring mainly on the 2−20 ps time scale. This is followed by a recombination in which ca. 80% of the ground-state reactants are regenerated within 1 ns. A photoelectrochemical device, prepared with a nanocrystalline NiO electrode coated with the phosphorus porphyrin, yields a cathodic photocurrent indicating that electrons indeed flow from the NiO electrode toward the solution. The low incident-to-photocurrent efficiency (IPCE) can be rationalized by the rapid back recombination reaction between the reduced sensitizer and the injected hole which prevents an efficient regeneration of the sensitizer ground state from the iodide/triiodide redox mediator. To the best of our knowledge, this work represents the first example of a photovoltaic cell in which a mechanism of hole photoinjection has been characterized.

Introduction

Considerable research efforts have been devoted to the design and the study of dye-sensitized semiconductor solar cells (DSSCs).[1] However, the majority of the reported studies are based on the sensitization of a n-type semiconductor (SC) which is generally titanium dioxide.[1,2] Surprisingly, until now, there are very few studies on the inverse process, namely, the photosensitization by hole injection into the valence band of a wide band gap p-type SC.[3−6] There are, however, many interesting reasons to investigate this process. First, from a fundamental viewpoint, it could be useful to identify and understand the parameters that govern the efficiency of hole injection from a photoexcited sensitizer grafted on a p-type SC. Second, this knowledge is important for a rational design of an efficient photovoltaïc device based on this principle. Furthermore, this latter photovoltaic cell requires the utilization of sensitizers displaying favorable oxidant excited-state properties rather than reductant excited-state properties, this makes it possible to use new chemical dyes that were not suitable for n-type DSSCs. Finally, this development may also provide an entry to the preparation of a tandem solar cell[5] consisting of a photosensitized anode such as TiO_2 and a photosensitized cathode such as the system studied here.

The p-type semiconductor used in this work is NiO, because its metal oxide nature permits it to firmly graft the sensitizer on its surface through carboxylic acid anchoring groups. Second, nanocrystalline transparent electrodes can be prepared with nickel oxide.[4,7] As a pre-study for this work, we have investigated NiO mesoporous films sensitized with coumarin 343 by femtosecond transient absorption spectroscopy, to verify that the desired interfacial electron-transfer dynamics could be obtained and studied in sensitized NiO films.[6] The sensitizer at the focus of the present investigation is instead a phosphorus porphyrin featuring axial ligands bearing a carboxylic group. While the coumarin was suitable for the fundamental studies of interfacial electron transfer, porphyrins and other tetrapyrroles are more attractive as dyes for a DSSC because of their better absorption in a large part of the visible spectrum. Furthermore, phosphorus porphyrin is known to be relatively easy to reduce[8−10] and to have quite a high energy excited state,[10] which renders this molecule suitable to photoinject a hole into the valence band of nickel oxide. In this paper, we report the characterization of the photophysical properties of a phosphorus porphyrin in solution and chemisorbed on a nickel oxide nanoporous film. The performance of a photovoltaic device based on a nickel oxide electrode coated with a phosphorus porphyrin is also reported.

Experimental Section

^{1}H NMR spectra were recorded on a Bruker or an Avance 300 MHz or an ARX 400 MHz spectrometer. Chemical shifts for ^{1}H NMR spectra are referenced relative to residual protium in the deuterated solvent ($CDCl_3$ = 7.26 ppm). Fast atom bombardement mass spectroscopy (FAB-MS) analyses were performed in a *m*-nitrobenzyl alcohol matrix (MBA) on a ZAB-HF-FAB spectrometer. UV−vis absorption spectra were re-

* To whom correspondence should be addressed. Fax: +46 18 471 3654. E-mail: Leifh@fki.uu.se. Fax: +33 2 51 12 54 02. E-mail: Fabrice.Odobel@univ-nantes.fr.
[†] Uppsala University.
[‡] Faculté des Sciences et des Techniques de Nantes.
[§] Royal Institute of Technology.

10.1021/jp054034a CCC: $30.25
Published on Web 11/10/2005

SCHEME 1. Preparation of the Phorphyrin Porphyrin Sensitizer 3[a]

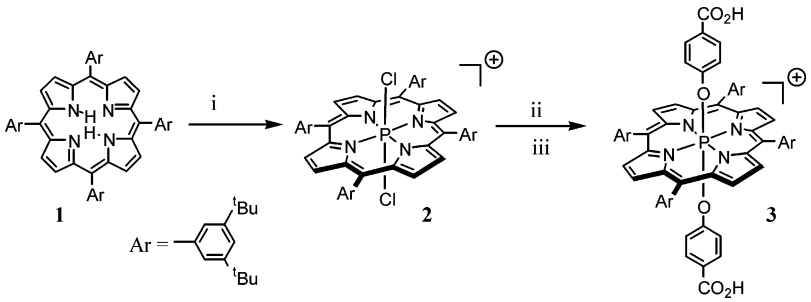

[a] Reagents and conditions: (i) $POCl_3$, pyridine, reflux (72%), (ii) 4-hydroxybenzoic acid, pyridine, reflux (35%), and (iii) CH_2Cl_2, HCl (92%).

corded on a UV-2401PC Shimadzu spectrophotometer. Fluorescence spectra were recorded on a SPEX Fluoromax or Flourolog II fluorimeter and were corrected for the wavelength-dependent response of the detector system.

The electrochemical measurements were performed with a potentiostat-galvanostat MacLab model ML160 controlled by resident software (Echem v1.5.2 for Windows) using a conventional single-compartment three-electrode cell. The working electrode was a Pt wire 10 mm long, the auxiliary was a Pt wire, and the reference electrode was the saturated potassium chloride calomel electrode (SCE). The supported electrolyte was 0.15 M Bu_4NPF_6 in dichloromethane, and the solutions were purged with argon before the measurements. All potentials are quoted relative to SCE. In all the experiments, the scan rate was 100 mV/s for cyclic voltammetry and 15 Hz for pulse voltammetry.

Time-resolved fluorescence was studied with a time-resolved correlated single photon counting system described previously.[11] Excitation was performed with ca. 120 fs laser pulses at 400 nm, and the emission was collected at magic angle polarization (55.4°) using suitable filters. The instrument response function was ~60 ps (fwhm). The laser system for transient absorption pump−probe experiments have been previously described.[12] Briefly, ~120 fs, 1 μJ laser pulses at 1 kHz were used for pumping (<2 μJ/pulse), and the probe continuum was generated from the fundamental in a rotating CaF_2 plate. The probe beam was divided in probe and reference, focused at overlap with the pump beam in a vertically moving 1 × 10 mm cell, spatially divided on an optical diffraction grating, and detected by a double diode array. To adjust for differences in laser intensity, the reference beam passed to the detector without going through the sample. A mechanical chopper blocked every second pump beam, and the transient absorption was calculated for every pair of pulses (not chopped/chopped) as $\Delta abs = -\log[(I_{probe,\tau=t}/I_{reference,\tau=t})/(I_{probe,\tau<0}/I_{reference,\tau<0})]$, where $\tau < 0$ refers to the pulses in which the pump light was chopped. The reported values are averages of 5000−10 000 individual measurements.

Time-resolved emission and transient absorption data on the μs time scale was collected with a frequency tripled Q-switched Nd:YAG laser. The output light pumped an optical parametric oscillator (OPO) delivering <10 ns flashes at 460 nm with an energy of ~15 mJ. An Applied Photophysics laser flash photolysis spectrometer was used to measure the time-resolved emission and transient absorption. The concentration of the solution samples was chosen so that the absorption at the excitation wavelength was around 0.1 and 0.4 for emission and transient absorption, respectively. For emission measurements on **3** attached to the NiO film, the sample surface was at ca. 10° angle relative to the excitation beam.

Thin-layer chromatography (TLC) was performed on aluminum sheets precoated with Merck 5735 Kieselgel $60F_{254}$. Column chromatography was carried out either with Merck 5735 Kieselgel 60F (0.040−0.063 mm mesh) or with SDS neutral alumina (0.05−0.2 mm mesh). Air-sensitive reactions were carried out under argon in dry solvents and glassware. Chemicals were purchased from Aldrich and used as received. 5,10,15,20-tetrakis(3,5-di*tert*butylphenyl)porphyrin **1** was prepared according to the literature method.[13]

Nanocrystalline NiO films were prepared on microscope glass or conducting glass (TEC8, SnO_2/F-coated glass, obtained from Hartford Glass) using methods described elsewhere.[7] The film thickness was typically 1 μm.

(5,10,15,20-Tetrakis(3,5-di*tert*butylphenyl)porphyrinato) Dichlorophosphorus(V) 2. $POCl_3$ (1.5 mL) was added dropwise to a solution of porphyrin **1** (0.5 g) in pyridine (7.5 mL), and the resulting solution was heating at reflux temperature for 48 h. The pyridine and the excess $POCl_3$ were removed under low pressure leaving a purple solid. This was dissolved in a minimum of dichloromethane and chromatographed on silica gel. Elution with dichloromethane/methanol 90/10 removed a pale red band containing unreacted free base porphyrin (0.24 g) and desired product (0.23 g). The solvent was removed to give the product as fine purple crystals (yield = 41%).

^{1}H NMR ($CDCl_3$): 9.11 (d, 8H, J = 9.12 Hz), 7.80 (s, 4H), 7.76 (s, 8H), 1.32 (s, 72H).

(5,10,15,20-Tetrakis(3,5-di*tert*butylphenyl)porphyrinato) Di(4-phenoxy carboxylic acid) Phosphorus(V) 3. Porphyrin **2** (0.15 g), 4-hydroxybenzoic acid (1.21 g, 70 equiv), in pyridine (50 mL) was heating at 145 °C for 5 days. The solvent was removed, and the crude product was chromatographed on silica gel with dichloromethane/methanol, 99.5/0.5. The solvent was removed to give the product as fine green crystals (yield = 35%).

^{1}H NMR ($CDCl_3$): 8.92 (d, 8H, J = 6.92 Hz), 7.68 (s, 4H), 7.44 (s, 8H), 6.62 (d, 4H, J = 15.82 Hz), 3.05 (s, 2H), 2.17 (d, 4H, J = 17.82 Hz), 1.26 (s, 72H). FAB-MS Calcd for $C_{90}H_{102}O_6N_4P$: 1366.75 ($M^{\bullet+}$). Found: 1366.7.

Results

Preparation of the Sensitizer. The insertion of phosphorus in the porphyrin core was accomplished according to the classical protocol[14] consisting of refluxing porphyrin **1** in a solution of phosphorus oxychloride in pyridine. The chloro axial ligands were subsequently replaced by carboxylic acid phenoxy groups by refluxing **2** with a large excess of 4-hydroxybenzoic acid to give **3** with 35% yield (Scheme 1).[10,15] After chromatography, the sensitizer **3** gave satisfactory analyses.

Electronic Absorption Spectrum. The absorption spectra of phosphorus porphyrin **3** in dichloromethane solution and after chemisorption on a NiO film are shown in Figure 1. The spectroscopic characteristics are gathered in Table 1.

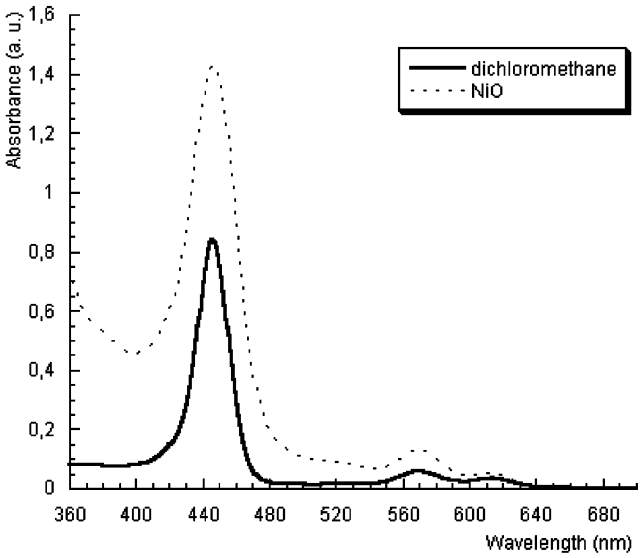

Figure 1. Absorption spectra of **3** in dichloromethane solution (straight line) and on NiO electrode (dotted line).

TABLE 1: Spectroscopic Characteristic of the Phosphorus Porphyrin 3 Recorded at Room Temperature

	absorption	emission	
	λ_{max}/nm (ϵ/M^{-1}cm^{-1})	λ_{max}/nm	τ_{max}/ps
3 in CH_2Cl_2	446 (1.21×10^5), 568 (9.2×10^3), 615 (5.50×10^3)	634, 687	3400
3 on NiO	446, 568, 613	[a]	<50
3 mono reduced in CH_2Cl_2	444 (5.1×10^4), 657 (4.6×10^3), 723 (5.8×10^3)		

[a] No emission detected.

After a few hours of immersion in a CH_2Cl_2 solution of **3**, the NiO electrode adopted a green coloration that clearly evidenced the effective adsorption of the sensitizer on its surface. The attachment of the dye was relatively strong since abundant rinsing of the film with dichloromethane did not result in any desorption of the sensitizer. Porphyrin **3** displays the usual intense Soret (at 446 nm) and Q-bands (at 568 and 613 nm) of regular porphyrins with absorbance maxima at similar positions as those reported previously for aryloxo phosphorus porphyrins.[9,10,16] The latter transition contains a charge-transfer character corresponding to a shift of electron density from the aryloxy axial ligand to the porphyrin macrocycle.[10,16] Such an intramolecular charge-transfer character could be favorable for hole injection into NiO from the anchoring axial ligand.

The spectrum of dye **3** is almost not altered upon its adsorption to the NiO film, indicating that no significant aggregation occurred on the electrode and that the electronic interactions between porphyrin and NiO are relatively weak (Figure 1 and Table 1). The sensitized electrode displays a strong absorbance at 446 nm due to the high molar extinction coefficient of the Soret band while the absorbance in the Q-band region is relatively weak. It can be expected that use of a thicker NiO film and addition of light scattering material will improve significantly the absorbance on the whole spectrum, most notably in the Q-band region.

Electrochemistry and Spectroelectrochemistry. The $P^+/P^\bullet$ reduction potential of phosphorus porphyrin **3** was measured by cyclic voltammetry in dichloromethane at room temperature. This process is reversible ($\Delta E = 80$ mV), and it occurs at -0.60 V vs SCE in agreement with the reported values of other phosphorus porphyrins.[10]

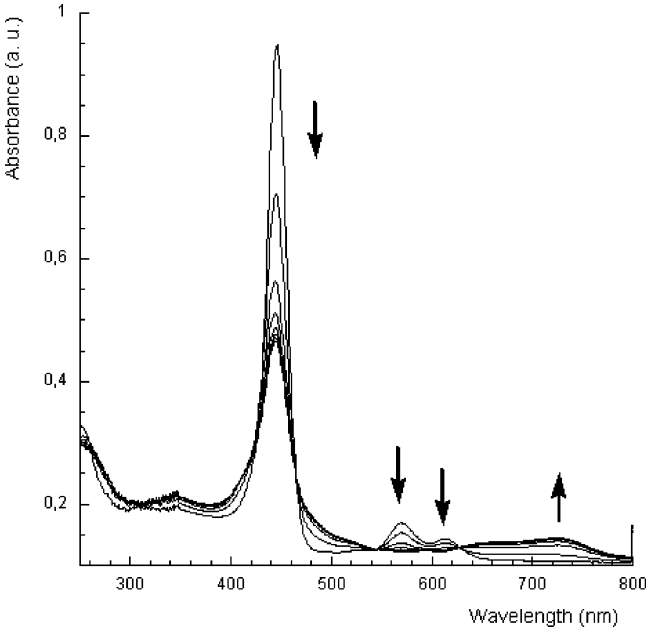

Figure 2. Spectral changes during the reduction of porphyrin **3** at -0.8 V vs SCE in dichoromethane containing 0.15 M of Bu_4NPF_6.

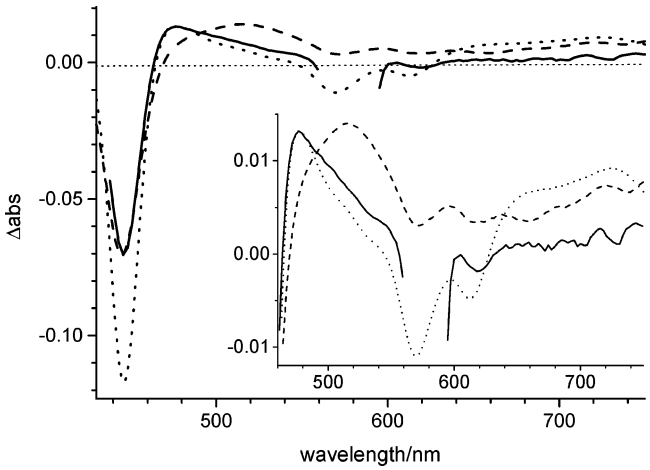

Figure 3. Normalized transient absorption spectra of **3** in CH_2Cl_2 for the singlet excited state (solid line) and the triplet exited state (dashed line) recorded at 5 ps and 8 ns, respectively, after excitation at 570 nm. The dotted line is the reduced minus the ground state difference spectrum obtained by spectroelectrochemistry. The inset shows the region above 460 nm on a magnified scale. The spectra are normalized at their respective transient absorption maxima.

Figure 2 shows the spectral changes during the electrochemical reduction of **3** performed at -0.8V vs SCE. When the porphyrin is reduced to produce the corresponding neutral radical, the intensity of the Soret band and the Q-bands decrease and a broad band appears between 620 and 800 nm instead. These spectral changes are in agreement with those reported by Kadish and co-workers on octalkylphosphorus phorphyrin and are indicative of a ring-centered π-anion radical.[8] The initial spectrum was totally recovered after reverse electrolysis at 0 V in agreement with a fully reversible reduction process. The difference spectrum ($P^\bullet - P^+$) is shown in Figure 3, and the differential extinction coefficients can be calculated from the data in Figure 3 (assuming complete electrochemical conversion) and the ground-state extinction coefficients (Table 1).

Emission Properties. The fluorescence spectrum of **3** in CH_2Cl_2 showed a strong fluorescence with emission maxima at 630 and 680 nm, typical for regular porphyrins. The

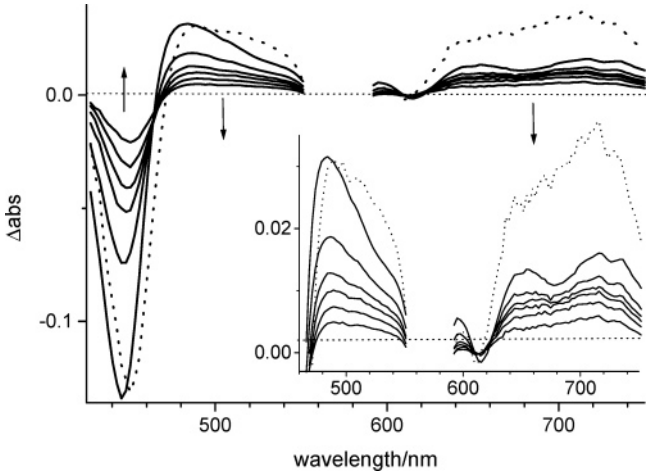

Figure 4. Transient absorption spectra of **3** attached to NiO film following 570 nm excitation. The spectra are recorded at 1 ps, 10 ps, 25 ps, 50 ps, 100 ps, and 1.5 ns after excitation, respectively. The dotted line shows the 1.5 ns spectrum normalized. The inset shows the region above 460 nm on a magnified scale.

fluorescence lifetime was 3.4 ns, similar to that for other regular porphyrins such as ZnTPP.[17] When attached to a NiO film, however, the emission was strongly quenched. Although it is difficult to quantify emission yields from molecules on such films relative to solution samples, the complete absence of detectable emission in both steady-state and time-resolved experiments suggest a >99% quenching and a <50 ps fluorescence lifetime. From this result, it can be concluded that the attachment of **3** on a NiO surface imparts a fast deactivation of the porphyrin singlet excited state.

Transient Absorption Measurements. To determine the nature of the deactivation processes of **3**, transient absorption spectroscopy was performed. The transient spectra of the singlet and triplet excited states of **3** in CH_2Cl_2 solution, recorded at 5 ps and 8 ns, respectively, after the excitation at 570 nm, are shown in Figure 3. The triplet spectrum recorded with a nanosecond flash photolysis setup was in good agreement with that in Figure 3 and decayed with a lifetime of ~30 μs in argon purged CH_2Cl_2. Also shown in Figure 3 is the difference spectrum ($P^\bullet - P^+$) for formation of the reduced porphyrin **3** in the spectroelectrochemical measurements (dotted line). This is normalized to give the same amplitude at the maximum as the singlet spectrum. In reality, the difference absorption for the radical ($\Delta\epsilon_{475} \approx 8 \times 10^3\ M^{-1}\ cm^{-1}$ from the spectroelectrochemical data) is probably much smaller than that for the excited states, as suggested by the relative magnitude of the Soret and Q-band bleach and by comparisons with the differential extinction coefficient for the excited singlet state of, for example, ZnTPP.[18] As the porphyrin radical spectrum in Figure 2 is flat in the Q-band region, the relative transient absorption magnitude of the different porpyrin states in Figure 3 was estimated by assuming that the Q-band bleach magnitude is the same in all states. The result suggests that the transient maximum around 480 nm is about 2.5−3 times smaller for the radical than that for the singlet excited state. Nevertheless, both the radical and triplet states display a pronounced absorption above 600 nm, while the singlet excited state shows stimulated emission around 670 nm.

When **3** was attached to a NiO electrode and excited with 570 nm light, the transient spectrum at early times is in perfect agreement with that from the singlet excited state in solution (Figure 4). At longer time delays, this spectrum decayed, and after 8 ns, the Soret band bleach had recovered by 90% (Figure 4). A global fit to the time evolution of the spectra over 12 characteristic wavelengths gave good residuals only when a sum of four exponential terms and a baseline offset was used, giving the following results: $\tau_1 = 2.8$ ps, $\tau_2 = 12.6$ ps, $\tau_3 = 55$ ps, $\tau_4 = 2500$ ps, and $\tau_5 > 10$ ns (baseline). The amplitude spectra for the respective components all showed porphyrin characteristics, with a higher relative absorption above 600 nm for the 2500 ps and >10 ns components. For the bleach recovery in the Soret band, the respective amplitudes for the components were $A_1 \sim 35\%$, $A_2 \sim 35\%$, $A_3 \sim 15\%$, $A_4 \sim 9\%$, and $A_5 \sim 6\%$.

The spectra in Figure 4 show that the stimulated emission disappears in tens of picoseconds meaning that the two shortest exponents and possibly the third are responsible for quenching of the singlet excited state. The extensive recovery of the Soret band absorption on the same time scales also implies that a large part of the quenching is followed by rapid ground-state repopulation. However (assuming that the Soret band bleach is similar for all intermediate states), in ca. 20% of the molecules, the singlet excited states are converted to a third state or states, and because these states have pronounced absorption above 600 nm, it is likely that it is either the triplet excited state or the reduced state, the latter meaning that an electron has been transferred from the NiO film into the porphyrin.

The dashed line in Figure 4 shows the transient spectrum at 1500 ps but normalized to the amplitude of the singlet excited state spectrum at 1 ps. The 1500 ps spectrum is clearly different from that of the singlet. Instead, it may possibly be attributed to the charge transfer state $P^\bullet - |NiO|^+$. The oxidized NiO spectrum is essentially flat in the spectral region of Figure 4, with $\Delta\epsilon \approx 6 \times 10^3\ M^{-1}\ cm^{-1}$ around 500 nm.[7] The addition of this spectrum to the $P^\bullet - P^+$ difference spectrum of Figure 3 gives a result that is in good agreement with the observed spectral shape after 1500 ps. The agreement between the relative absorption magnitudes in the Soret band bleach and the absorption around 480 and 700 nm nm is within experimental error, and the addition of the oxidized NiO spectrum to the $P^\bullet - P^+$ difference spectrum lifts also the expected Q-band bleach features above the baseline, as observed in the time-resolved spectra of Figure 4. The maximum at 485 nm is 10 nm red shifted compared to the $P^\bullet - P^+$ difference spectrum, possibly because of the attachment to NiO. Because of the similarity of the spectra for the different states, however, we cannot exclude that at least one part of the 1500 ps spectrum is due to the porphyrin triplet state. This state lies ca. 0.3 eV below the corresponding singlet state, but far above the charge transfer state, and must in that case have been formed directly from the singlet, with a low yield. The rapid and efficient quenching of the latter, as observed in the emission and transient absorption experiments, means that triplet formation should be negligible, unless intersystem crossing is enhanced by paramagnetic nickel centers in the NiO film. Moreover, the shape of the band in the 470−540 nm region is very similar to the $P^\bullet - P^+$ difference spectrum, with a sharp increase on the blue side, while the triplet band is more symmetric and red shifted. Finally, the similar transient absorption magnitude of the bands around 480 and 700 nm, respectively, is in good agreement with a sum of the $P^\bullet - P^+$ and the $|NiO|^+ -$ NiO difference spectra, while the absorption around 700 nm in the triplet spectrum is relatively small (Figures 3−4). Thus, we favor the interpretation that at least most of the species giving the transient absorption at 1500 ps is the $P^\bullet - |NiO|^+$ state. This is supported by the observation of a photocurrent in the photoelectrochemical experiments below.

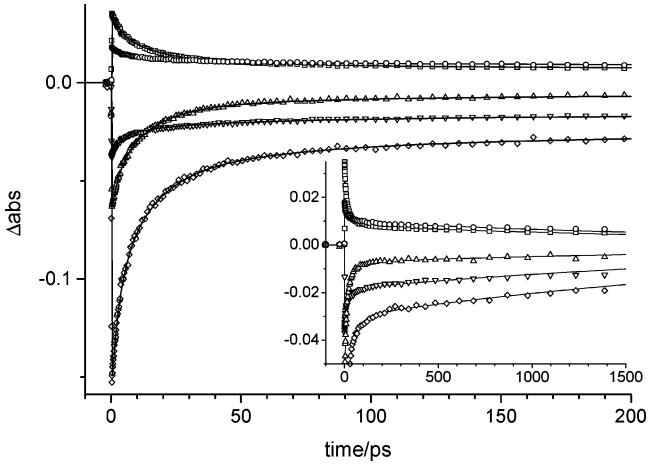

Figure 5. Transient absorption traces of **3** attached to NiO film following 570 nm excitation and probed at 430 nm (up triangles), 445 nm (diamonds), 461 nm (down triangles), 485 nm (squares), and 715 nm (circles), respectively. The solid lines are least-squares fits to the data with four exponentials and a baseline offset: $\tau_1 = 2.8$ ps, $\tau_2 = 12.6$ ps, $\tau_3 = 55$ ps, and $\tau_4 = 2500$ ps. The inset shows the same data on a longer time scale.

The estimate above of ca. 80% ground-state recovery within 1 ns, based on the Soret band recovery, is then probably somewhat incorrect, as the $P^{\bullet} - |NiO|^+$ absorption is substantial in this region (Figure 2). From the relative absorption around 480 nm of the $P^{\bullet} - |NiO|^+$ and excited singlet states estimated above, it seems that somewhere between one-fourth and one-half of the initially excited porphyrins are in the $P^{\bullet} - |NiO|^+$ state after 1500 ps. Although rapid recombination to the ground state must occur on a time scale overlapping with that for the initial hole injection, a significant fraction thus remains on a nanosecond time scale. Recombination on a range of time scales is also observed for the dye$-|TiO_2|$ systems.[19]

To possibly detect the fraction of light-induced species more long-lived than 10 ns, nanosecond flash photolysis was carried out. Excitation at 570 nm resulted in a difference absorption spectrum with a small amplitude (only ca. 1% of the initially excited molecules, not shown) but with clear porphyrin characteristics decaying on the 100 ns to 10 μs time scale. Possibly part of this is due to a small fraction of more long-lived reduced porphyrin undergoing recombination in the $P^{\bullet} - |NiO|^+$ state. The small signal and the similarity between the reference spectra, however, precluded an unambiguous assignment to the $P^{\bullet} - |NiO|^+$ state. In any case, the results show that under these experimental conditions only a very small fraction of charge-separated states are still present after 20 ns.

Photoelectrochemistry of Dye-Sensitized Nanocrystalline NiO Electrodes. Nanocrystalline NiO electrodes coated with phosphorus porphyrin **3** were assembled in a "sandwich" solar cell, using platinized conducting glass as the counter electrode. A redox electrolyte containing the iodide$-$triiodide redox couple filled the space between the electrodes. Upon illumination with white light, a cathodic photocurrent was observed, that is, electrons were transferred from the dye-sensitized NiO electrode to the electrolyte. The incident photon-to-current conversion efficiency (IPCE) was recorded as a function of the excitation wavelength (Figure 6). The resulting photocurrent action spectrum clearly reveals the features of the absorption spectrum of the sensitizer, indicating that the phosphorus porphyrin is the photoactive species at the origin of the photocurrent. IPCE values were rather modest. The highest value (2.5%) was found at the most intense absorption in the Soret band. The dye absorbance of this sample was about 0.45 au at this maximum

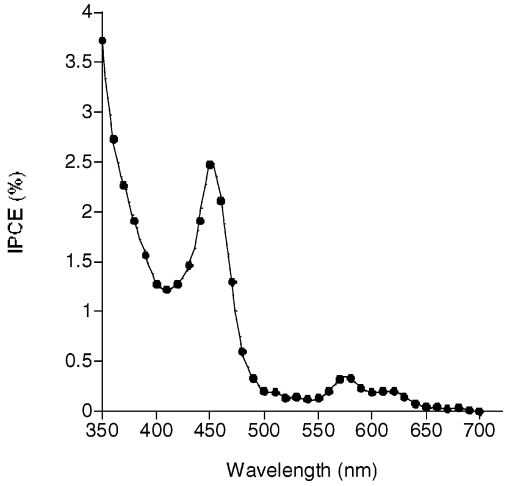

Figure 6. Photocurrent action spectrum of nanostructured NiO electrode (thickness 800 nm) coated with phosphorus porphyrin **3**. The electrolyte is composed of 0.5 M NaI and 0.05 M I_2 in propylene carbonate.

SCHEME 2. Energetic Diagram of the NiO Photoanode Sensitized by Phosphorus Porphyrin 3[a]

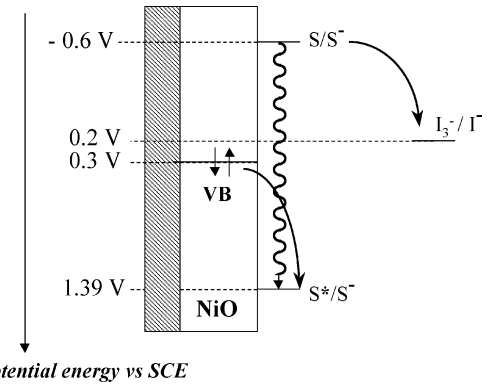

[a] VB, valence band of NiO; S, sensitizer.

in the sensitized NiO film, so that about 65% of the incoming light is absorbed. Under open circuit conditions, the dye-sensitized NiO electrode develops a positive photovoltage with respect to the counter electrode, which is rather small (<100 mV).

Discussion and Conclusions

A relatively easy-to-prepare sentitizer has been synthesized through two steps from usual free base porphyrin. Determination of the redox potential and the energy of the singlet excited state of phosphorus porphyrin enables us to calculate an estimate for the free energy of an excited-state hole injection with eq 1

$$\Delta G^0 = eE^0_{VB}(NiO) - [E_{00}(\mathbf{3}) - eE^0_{red}(\mathbf{3}^+/\mathbf{3}^-)] \quad (1)$$

where e is the elementary charge, $E^0_{VB}(NiO)$, $E_{00}(\mathbf{3})$, and $E^0_{red}(\mathbf{3}^+/\mathbf{3})$ denote the valence band potential of NiO, the singlet excited-state energy of porphyrin **3**, and the reduction redox potential of **3**, respectively. $E^0_{VB}(NiO)$ was reported[4] to be equal to 0.3 V vs SCE, $E_{00}(\mathbf{3}) = 1.99$ eV was determined from the wavelength at the intersection of the absorption and emission spectra (624 nm), and $E^0_{red}(\mathbf{3}^+/\mathbf{3}) = -0.6$ V was determined here by cyclic voltammetry. The calculated driving force for the hole injection is very large, $\Delta G^0 = -1.1$ eV, so that this process is very favorable from a thermodynamic point of view. An energetic diagram of the redox processes involved in this photovoltaic device is illustrated in Scheme 2. Note that electron

transfer involving also the higher excited porphyrin S_2 state obtained by Soret band excitation is in principle possible, as has been demonstrated in Zn^{II} porpyrin−acceptor assemblies.[12,20] However, whereas the S_2 state has ca. 2 ps lifetime in, for example, ZnTPP, we observed no spectral changes attributable to S_2-to-S_1 conversion in the phosphorus porphyrin **3** on the time scale comparable to the electron transfer from NiO. This suggests a much more short-lived S_2 state that will not undergo significant electron transfer prior to S_2-to-S_1 relaxation.

In the following paragraphs, we discuss the reason for the relatively poor IPCE values obtained in the DSSC experiments (Figure 6). The IPCE is essentially controlled by three factors: the light harvesting efficiency (LHE), the hole injection quantum yield (Φ_{inj}), and the charge collection efficiency at the ITO electrode (η_{cc})

$$\mathrm{IPCE} = \mathrm{LHE} \times \phi_{inj} \times \eta_{cc} = \mathrm{LHE} \times \phi_{inj} \times \phi_{esc} \times \eta_{tr} \quad (2)$$

It is useful to separate the charge collection efficiency in two terms for the two types of recombination that occur: with the reduced dye and with the reduced form of the redox pair. ϕ_{esc} represents the escape quantum yield, which is the probability that an injected hole does not recombine with the reduced dye directly. It depends strongly on the regeneration rate of the reduced dye to its normal state by the redox couple. The transport efficiency η_{tr} is the probability that the hole reaches the conducting substrate, rather than reacting with the electrolyte. In the Soret band (446 nm), the LHE is high (65%). Φ_{inj} is relatively high since on NiO the porphyrin fluorescence is completely (>99%) quenched. Furthermore, the transient absorption data suggest that the quenching is at least mainly due to hole injection from the excited dye into the valence band of NiO, forming the $P^{\bullet} - |NiO|^{+}$ state. Therefore, η_{cc} appears to be the main factor responsible for the low efficiency of the cell. To determine whether this is due to low values of either ϕ_{esc} or η_{tr} (eq 2), we note the following: First, the transient absorption data suggest that recombination to the ground state occurs on a range of time scales from picoseconds to nanoseconds and, after ca. 20 ns, at most a few percent of the charge-transfer state remains. In this respect, there was only a marginal improvement compared to the previous coumarin 343−NiO system.[6] Second, the regeneration of the reduced dye by the triiodide was not measured, but it is probably not much faster than about 10 ns, which is the typical time scale for regeneration of the oxidized dye in the conventional dye-sensitized TiO_2-based solar cells,[21] although the occurrence of faster reactions between preformed porphyrin−triiodide complexes cannot be excluded. Note also that the reduction of triodide into iodide is known to be slow without a catalyst.[22] It seems obvious, therefore, that the electrolyte can compete with recombination only to a small extent, so that ϕ_{esc} will be rather small in the P-porphyrin−NiO system. Finally, the shape of the IPCE spectrum gives an indication about the charge transport efficiency.[23] The resemblance of the IPCE spectrum with the LHE spectrum shows that the probability for an injected hole to reach the conducting substrate is similar in the whole film. Specifically, the ratio between Soret and Q-bands is nearly identical in IPCE and LHE spectra, although light in the strongly absorbing Soret band region will to a large extent be absorbed close to the irradiated surface, while excitation in the Q-band regions will be spread more evenly in the film. It thus appears that η_{tr} is close to 1 and that the main factor behind the low IPCE value, even in the Soret band region where the LHE is high, is instead the rapid recombination reaction between the reduced dye and holes in the valence band of NiO.

Direct transient absorption measurements on the complete cells were precluded by the strong absorption of the electrolyte in the relevant spectral regions. In particular, we could not hope to resolve any reaction with the electrolyte, which according to the IPCE values would correspond to only ca. 2.5% of the overall reaction. Nevertheless, the very rapid and efficient quenching of the excited porphyrin by the NiO film strongly suggest that the primary quenching mechanism is hole injection also in the photovoltaic cell, as excited-state electron transfer to the electrolyte is not likely to compete kinetically on the 1−10 ps time scale. Note that reports of oxidative quenching of porphyrins by I_3^- have instead concerned much more long-lived excited states ($\tau \approx 1$ ns).[24] In our experiments, instead, it is much more likely that electron transfer to I_3^- will occur from the large fraction (25−50%, see above) of $P^{\bullet}$ observed after 1.5 ns (Figure 4) and compete with recombination with the holes in the semiconductor. Thus, we attribute the observed photocurrent to a photovoltaic process in which the primary reaction is hole injection from the singlet excited porphyrin **3** to the NiO film. Clearly, the electrolyte employed is far from optimal in the present system but was used for this demonstration of a p-type DSSC. Further efforts must include a search for a better electrolyte, as has been done extensively for the dye−TiO_2 system[2] but also a dye−p-type semiconductor system that shows a slower recombination reaction. Nevertheless, this is the first study of a p-type DSSC in which a good binding and rapid quenching of the dye by the semiconductor were established and the mechanism and dynamics of the interfacial electron transfer was addressed. As such, it is an important step toward the use of efficient photoactive cathodes in DSSC systems.

Acknowledgment. We thank Leonard Csenki for preparation of the nanocrystalline NiO films. This work was supported by The Swedish Foundation for Strategic Research, The Swedish Research Council, The Knut and Alice Wallenberg Foundation, and the "Action Concertée Incitative" (ACI) "Jeune Chercheur" 4057 financed by the French Ministry of Research. L.H. acknowledges a Research Fellow position from the Royal Swedish Academy of Sciences.

References and Notes

(1) Kalyanasundaram, K.; Grätzel, M. *Coord. Chem. Rev.* **1998**, *177*, 347−414.

(2) Grätzel, M. *Nature* **2001**, *414*, 338−344. Hagfeldt, A.; Grätzel, M. *Chem. Rev.* **1995**, *95*, 49. Hagfeldt, A.; Grätzel, M. *Acc. Chem. Res.* **2000**, *33*, 269−277.

(3) (a) Memming, R.; Tributsch, H. *J. Phys. Chem.* **1971**, *75*, 562−570. (b) Poznyak, S. K.; Kulak, A. I. *Electrochim. Acta* **1990**, *35*, 1941−1947. (c) Nakabayashi, S.; Ohta, N.; Fujishima, A. *Phys. Chem. Chem. Phys.* **1999**, *1*, 3993−3997. (d) O'Regan, B.; Schwartz, D. T. *J. Appl. Phys.* **1996**, *80*, 4749−4753. (e) O'Regan, B.; Schwartz, D. T. *Chem. Mater.* **1995**, *7*, 1349−1354.

(4) He, J.; Lindström, H.; Hagfeldt, A.; Lindquist, S.-E. *J. Phys. Chem. B* **1999**, *103*, 8940−8943.

(5) He, J.; Lindström, H.; Hagfeldt, A.; Lindquist, S. E. *Sol. Energy Mater. Sol. Cells* **2000**, *62*, 265−273.

(6) Morandeira, A.; Boschloo, G.; Hagfeldt, A.; Hammarström, L. *J. Phys. Chem. B* **2005**, *109*, 19403−19410.

(7) Boschloo, G.; Hagfeldt, A. *J. Phys. Chem. B* **2001**, *105*, 3039−3044.

(8) Akiba, K.-y.; Nadano, R.; Satoh, W.; Yamamoto, Y.; Nagase, S.; Ou, Z.; Tan, X.; Kadish, K. M. *Inorg. Chem.* **2001**, *40*, 5553−5567.

(9) Giribabu, L.; Rao, T. A.; Maiya, B. G. *Inorg. Chem.* **1999**, *38*, 4971−4980.

(10) Rao, T. A.; Maiya, B. G. *Inorg. Chem.* **1996**, *35*, 4829−4836.

(11) Johansson, O.; Borgström, M.; Lomoth, R.; Palmblad, M.; Bergquist, J.; Hammarström, L.; Sun, L.; Åkermark, B. *Inorg. Chem.* **2003**, *42*, 2908−2918.

(12) Andersson, M.; Davidsson, J.; Hammarström, L.; Korppi-Tommola, J.; Peltola, T. *J. Phys. Chem. B* **1999**, *103*, 3258−3262.
(13) Heitz, V.; Chardon-Noblat, S.; Sauvage, J.-P. *Tetrahedron Lett.* **1991**, *32*, 197−198.
(14) Marrese, C. A.; Carrano, C. J. *Inorg. Chem.* **1983**, *22*, 1858−1862.
(15) Segawa, H.; Kunimoto, K.; Nakamoto, A.; Shimidzu, T. *J. Chem. Soc., Perkin Trans. 1* **1992**, 939−940.
(16) Susumu, K.; Tanaka, K.; Shimidzu, T.; Takeuchi, Y.; Segawa, H. *J. Chem. Soc., Perkin Trans. 2* **1999**, 1521−1529.
(17) Kalyanasundaram, K. *Photochemistry of polypyridine and porphyrin complexes*; Academic Press: London, 1992.
(18) Rodriguez, J.; Kirmaier, C.; Holten, D. *J. Am. Chem. Soc.* **1989**, *111*, 6500−6506.
(19) Haque, S. A.; Tachibana, Y.; Willis, R. L.; Moser, J. E.; Graetzel, M.; Klug, D. R.; Durrant, J. R. *J. Phys. Chem. B* **2000**, *104*, 538−547.
(20) Hayes, R. T.; Walsh, C. J.; Wasielewski, M. R. *J. Phys. Chem. A* **2004**, *108*, 2375−2381. Mataga, N.; Chosrowjan, H.; Taniguchi, S. *J. Photochem. Photobiol., C* **2005**, *6*, 37−79.
(21) Pelet, S.; Moser, J.-E.; Graetzel, M. *J. Phys. Chem. B* **2000**, *104*, 1791−1795.
(22) Duffy, N. W.; Peter, L. M.; Rajapakse, R. M. G.; Wijayantha, K. G. U. *J. Phys. Chem. B* **2000**, *104*, 8916−8919.
(23) Boschloo, G. K.; Goossens, A. *J. Phys. Chem.* **1996**, *100*, 19489−19494.
(24) Splan, K. E.; Massari, A. M.; Hupp, J. T. *J. Phys. Chem. B* **2004**, *108*, 4111−4115.